Dispersion of a Solids Stream Falling into a Stationary Liquid

K. M. Smith[1], M. R. Davidson[1] and D.F. Fletcher[2]

1. G.K. Williams Cooperative Research Centre for Extractive Metallurgy, Department of Chemical Engineering, The University of Melbourne, Parkville, Vic., 3052, Australia.
2. Department of Chemical Engineering, University of Sydney, NSW, 2006, Australia.

ABSTRACT

In smelting processes, pelletised feed solids are frequently introduced as a continuous stream into a bath of molten liquid. A wide dispersion of feed solids within the melt increases their exposure to oxidising or reducing reagents. Thus an improved understanding of factors affecting such dispersion is desirable. Recent investigations in the computational modelling of a solids stream entering a stationary liquid, have successfully predicted the main features of steel particles dispersing in water (Fletcher and Witt, 1996). The model uses an Eulerian multiphase formulation with a non-diffusive convective differencing scheme. In this paper, those developments are applied to a cold model of a metallurgical flow. Predictions are obtained and discussed for a range of values of solid densities, inlet particle volume fractions, impact velocities and particle diameters.

NOMENCLATURE

B	Constant in eq. (6)
C_D	Drag Coefficient
d_s	Particle Diameter
F_D	Force due to Drag
Re_s	Particle Reynolds Number
V_l	Instantaneous Liquid Velocity
V_s	Instantaneous Particle Velocity
Vin	Inlet Particle Velocity

Greek symbols

α_l	Liquid Volume Fraction
α_s	Particle Volume Fraction
α_{smax}	Maximum Particle Volume Fraction
ρ_l	Liquid Density
μ_l	Liquid Viscosity
μ_m	Mixture Viscosity
μ_s	Solid Viscosity

1. INTRODUCTION

A number of metallurgical processes involve the entry of a solids stream into a liquid. Some examples include, the addition of fresh concentrate in the Noranda Process for the production of copper (George and Taylor, 1981), damp pellets of lead charge fed into the QSL reactor (Kellogg and Diaz, 1992), ferro-alloy or aluminium additions to ladles (Guthrie *et al.*, 1975), and the addition of lump coal into an Isasmelt smelter (Errington *et al.*, 1985; Nagamori *et al.*, 1994). Another process which is gaining increasing importance in the area of ferrous metallurgy is the use of direct reduced iron as a continuous charge in an electric arc furnace (Brown and Reddy, 1979).

Typically, solids entering a metallurgical system are of a density equivalent to or less than that of the liquid. In an Isasmelt smelter, for example, the density of lump coal is approximately 1,300 kg/m^3 (Incropera and DeWitt, 1990) whereas copper slag density is greater than 3,000 kg/m^3 (Biswas and Davenport, 1980). An electric arc furnace melt density approaches that of steel at 7,000 kg/m^3 (Peters, 1982) whilst direct reduced iron briquettes entering the furnace would have density approximately 5,500 kg/m^3 (Stephenson, 1980). Few experimental or computational results exist to describe the processes occurring when buoyant or near buoyant particles enter a liquid, although some single particle studies have been performed

(Guthrie *et al.*, 1975). Recent computational (Hall and Fletcher, 1995; Fletcher, 1995; Fletcher and Witt, 1996) and experimental (Gilbertson and Fletcher, 1992; Gilbertson, 1993) work considered high density spheres falling into water. This paper extends the computational model of Fletcher to buoyant particles. Modelling aspects of related studies and other research which focuses on fluid/particle interaction (Gidaspow, 1986; Bouillard *et al.*, 1989; Davidson, 1994) are implemented.

The purpose of this paper is to predict the penetration behaviour of a stream of buoyant, or near buoyant, solid particles entering a stationary liquid, representative of a metallurgical system under non-reacting conditions. Calculations are performed for a range of particle densities, diameters, inlet volume fractions and impact velocities.

2. BACKGROUND

2.1 The Model

A single layered two-dimensional system, shown schematically in Figure 1, is considered. Solids are assumed to enter with a known velocity and volume fraction. The flow is taken to be laminar.

In practice, a slag layer is present on the surface of a melt. As a first step the slag layer is ignored, with the solids assumed to pass through it unhindered. Heat transfer and particle dissolution within the melt are also not considered. The extension to a two-layered system with the eventual inclusion of heat and mass transfer will be the subject of future work.

Physical properties are chosen consistent with ferrous applications for which a liquid density of 7,000 kg/m^3 with a viscosity of 0.0064 Pa.s (Guthrie *et al.*, 1975; Peters, 1982) are assumed. The liquid properties are fixed thoughout the calculations.

Particle parameters to be varied are the density, diameter, inlet volume fraction and impact velocity. Particle densities range from 5,500 kg/m^3 to 8,500 kg/m^3, extending slightly beyond the neutrally buoyant point. The diameters are chosen between 0.01m - 0.05 m which encompasses typical direct reduced iron pellet sizes (Stephenson, 1980).

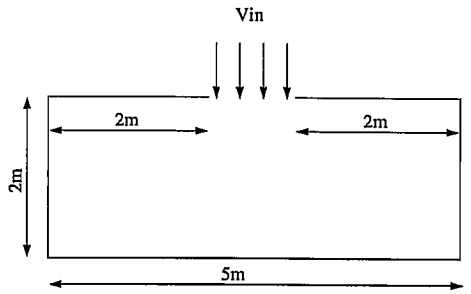

Figure 1 - Geometry of the Computational Domain

An appropriate choice of inlet volume fraction is not clear. The maximum volume fraction of particles, α_s, falling steadily in a stationary fluid (flooding condition) is about 0.2 (Zuber, 1964). This is close to the value of volume fraction in the experiments of Gilbertson *et al.* (1992) at release, after which the volume fraction was observed to reduce to 0.1 during a 0.1m fall. Typically, the solids will fall further than 0.1m during addition to a melt; thus α_s is varied between 0.03 and 0.15 here.

The impact velocity of solids is varied between 5 m/s and 20 m/s. This range encompasses velocity values quoted for direct reduced iron falling into an electric arc furnace, approximately 7-9 m/s (Stephenson, 1980). Generally, velocity is controlled by the release height of the particles above the melt surface.

2.2 The Model Equations

Transient two-phase flow calculations are performed using the fluid flow program CFX F3D (AEA Technology, 1995) utilising an Eulerian two-fluid approach in which the phases are regarded as interpenetrating continua. The momentum equations for both phases are adapted to include particle added mass and lift terms according to Fletcher and Witt (1996). The objective form of these terms is chosen, as given by Drew and Lahey (1987).

The standard drag force for spherical particles is modified to include hindered settling effects (e.g. Gidaspow, 1986; Davidson, 1994):

$$F_D = 150\frac{\alpha_s^2\mu_l}{\alpha_l d_s^2} + 1.75\frac{\rho_l|V_l - V_s|}{d_s}\alpha_s$$

for $\alpha_l \leq 0.8$ (1)

$$F_D = \frac{3}{4}C_D\frac{\alpha_s\alpha_l|V_l - V_s|\rho_l}{d_s}\alpha_l^{-2.7}$$

for $\alpha_l > 0.8$ (2)

with the drag coefficient

$$C_D = \max\left(0.44, \frac{24}{Re_s}\left(1 + 0.15Re_s^{0.687}\right)\right) \quad (3)$$

and the particle Reynolds number given by

$$Re_s = \frac{|V_l - V_s|d_s\alpha_l\rho_l}{\mu_l} \quad (4)$$

Equation (1) for larger solids fractions is based on the Ergun equation. For solid volume fraction less than 0.2, the standard drag relation for a single particle is modified for packing effects (2).

The presence of particles in a liquid modifies the overall mixture viscosity. This has been taken into account by the use of a variable solids viscosity, dependent upon the solids volume fraction. The mixture viscosity, defined as

$$\mu_m = \mu_l\alpha_l + \mu_s\alpha_s \quad (5)$$

is taken to be (Shook and Roco, 1991; p. 62)

$$\mu_m = \mu_l\left[1 - \frac{\alpha_s}{\alpha_{smax}}\right]^{-B\alpha_{smax}} \quad (6)$$

with B= 2.5, with α_{smax} = 0.63.
The solids viscosity follows from Equations (5) and (6).

2.3 Numerical Considerations

Previous work on computational modelling of spherical particles dropped into water (Fletcher and Witt, 1996) has shown the need for a total variation diminishing (TVD) convective differencing scheme (eg. van Leer, 1974) to ensure realistic predictions of the solids "plume". Fletcher and Witt showed that the use of a highly diffusive scheme, such as HYBRID, can cause excessive smearing of the interface between the liquid and the falling particles. The van Leer differencing scheme is applied in the present calculations.

Constant pressure is chosen on the top boundary either side of the solids column. The walls of the tank are all specified as no slip boundaries. To avoid an unphysically large initial impulse, the particle volume fraction is ramped from zero to the maximum value over 20 ms. Calculations are performed on a 125x50 rectangular grid with a timestep of 0.001 seconds. Refining the grid produces no significant difference in the predicted flow. Convergence is assumed when the sum of the normalised residuals of mass, and momentum are less than 10^{-6}. All two dimensional CFX F3D calculations are treated as three dimensional problems with one internal plane in the k-direction (AEA Technology, 1995), thus the tank width is set to 1 m.

3. RESULTS AND DISCUSSION

Particle parameters are varied around a base case of 15 m/s impact velocity with inlet volume fraction 0.05, particle diameter 0.03 m, and a particle density of 7,000 kg/m^3, equal to that of the liquid.

To prevent the solids volume fraction from attaining unrealistic values in excess of a value for maximum packing, a solids pressure can be introduced into the particle phase momentum equation. This represents a normal (dispersive) solids stress which arises from persistent particle-particle contacts. A suitable form of the solids pressure is given in Bouillard *et al.* (1989).

For the base case, the solids volume fraction achieves maximum packing values in approximately 0.15 s. The addition of a solids pressure term added to the particle phase momentum equation would justify the continuation of the calculation. However, at present timestepping is halted when the solids volume fraction reaches 0.63. The addition of this solids pressure will be explored in future work.

Figure 2 shows the contours of volume fraction of the base case at t = 0.15 s. It is seen that the particle "plume" is beginning to resemble that produced experimentally by Gilbertson *et al.* (1992), and Hall and Fletcher (1995), for high density stainless steel spheres in water at t = 0.16 s.

All contour diagrams of solid volume fraction are shown in intervals of 0.1, however, the diagrams also have a 0.02 interval shown. This value has been used to delineate the boundary between the liquid and the solid regions (Fletcher and Witt, 1996) when the particle penetration depth is calculated.

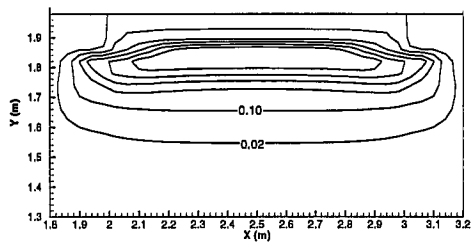

Figure 2-Contours of volume fraction for the base case at 0.15 s. Contour values are 0.02, 0.1 - 0.5.

3.1 The Effect of Particle Inlet Velocity

Particle impact velocity is varied between 5 m/s and 20 m/s whilst keeping the remaining base case parameters constant.

Decreasing the impact velocity decreases the speed of formation of the particle "plume", reducing the horizontal dispersion and penetration depth with respect to the base case. A reduction of impact velocity also causes the rate of increase of solids volume fraction at a given time to decline. This is a logical consequence of decreasing particle velocity since the number of particles in the tank is less. At time 0.15 s, the mass in the tank for the base case is ~735 kg. The equivalent mass is reached at 0.43 s for impact velocity of 5 m/s. The contours of volume fraction for this case are almost identical with Figure 2. This result suggests a possible advantage in introducing particles into the liquid more slowly. Lower volume fractions allow greater access to the particle by the liquid, therefore promoting solid dissolution. Practically, however, the reduction of impact velocity may not be feasible since the need for the particles to penetrate the slag layer necessitates a minimum velocity value (Stephenson, 1980).

Another consequence of increasing the particle impact velocity is an expected increase in depth of penetration defined as the lowest point on the centre line of the tank where the volume fraction of solids is 0.02. Figure 3 shows the depth of penetration vs time. Clearly particles can penetrate further into the liquid at higher velocities.

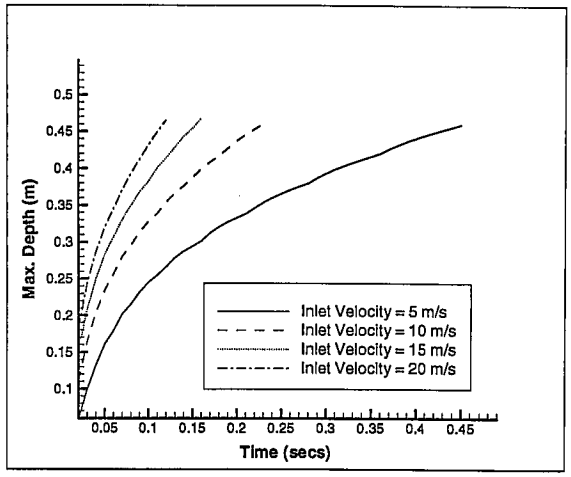

Figure 3-Particle depth vs time for various impact particle velocities. Values of volume fraction, particle density and particle diameter are those for the base case.

3.2 Particle Sizes Effects

Figure 4 shows the effect of increasing the particle diameter on the penetration depth. Solids with a particle diameter of 0.05 m are predicted to penetrate much more deeply into the liquid bath than those with smaller diameters. As a consequence, the volume

fraction contours are not as close together for greater particle diameters as shown in Figure 5, compared with volume fraction contours generated for the base case at the same time (figure 2). Larger diameter solids penetrate the liquid to a greater extent because they experience a lower drag force.

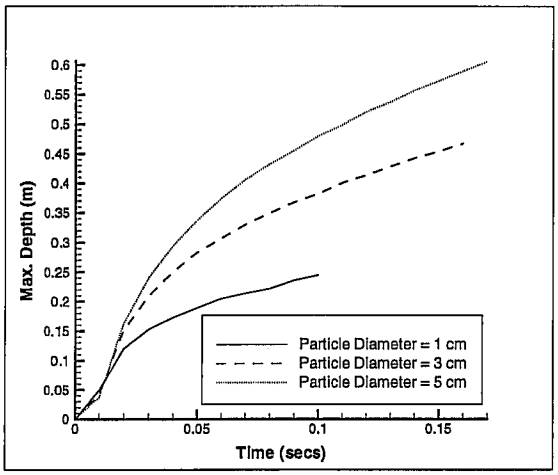

Figure 4 - Penetration depth vs time for various particle diameters. Values for volume fraction, particle density and impact velocity are those for the base case.

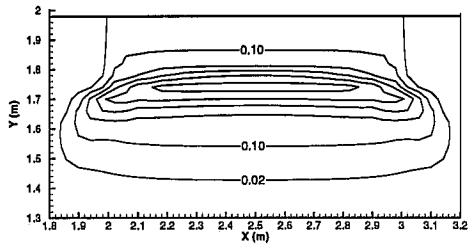

Figure 5 - Contours of volume fraction for increased particle diameter 0.05m at t = 0.15 s. Remaining parameters as in base case. Contour values are 0.02, 0.1 - 0.5.

3.3 Solid Density Effects

Three particle density calculations were performed with values of 8,500 kg/m^3, 5,500 kg/m^3 and the neutrally buoyant value of 7,000 kg/m^3. Figure 6 shows the effect of the particle density on the penetration depth of the particles, with higher density particles penetrating further into the liquid. This occurs because the high density particle have a larger gravitational force acting on them and a higher kinetic energy. However, for the range of particle densities chosen, the variation of particle depth is not as large as that due to changes in impact velocity (Figure 3) or changes in particle diameter (Figure 4). This indicates that the system is drag rather than gravity dominated for the present choice of solids parameters.

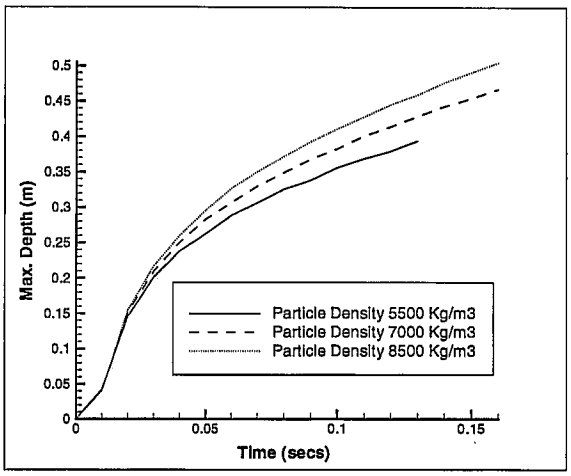

Figure 6 - Penetration depth vs time for various particle densities. Values for volume fraction, impact velocity and particle diameter are those for the base case.

3.4 Changing Inlet Solid Volume Fraction

Reducing the volume fraction of particles entering the inlet has a similar effect to decreasing the impact velocity. In both cases, the mass flow rate of charge entering the system is reduced, thereby reducing the volume fraction of solids present in the liquid at a given time.

The increase in particle volume fraction appears to have only a minimal effect on particle penetration depth with time (Figure 9), when compared with the figures for varying particle density, impact velocity and particle diameter. However, a comparison of Figures 7 and 8 shows that when the mass in the tanks is equal, the lower volume fraction case allows for greater particle penetration.

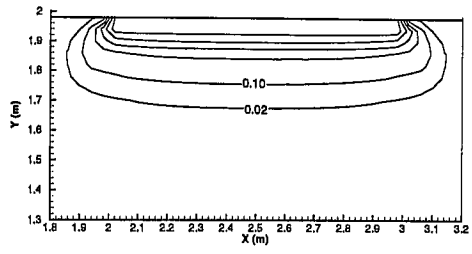

Figure 7 - Contours of volume fraction for α_s = 0.15 at t = 0.05 s, mass = 630 kg. Remaining parameters as in base case. Contour values are 0.02, 0.1 - 0.5.

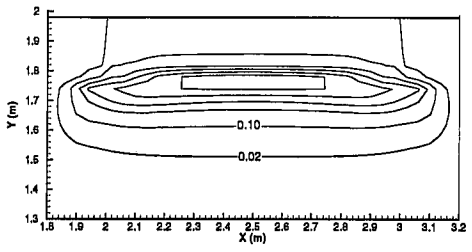

Figure 8 - Contours of volume fraction for α_s = 0.03, t = 0.21 s, mass = 630 kg. Remaining parameters as in base case. Contour values are 0.02, 0.1 - 0.5.

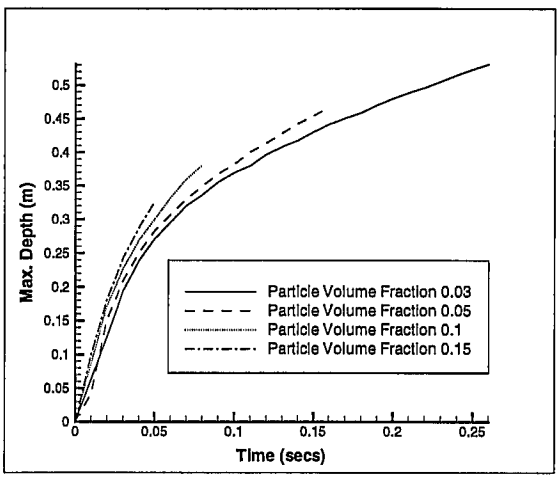

Figure 9 - Penetration depth vs time for various inlet volume fractions. Values for impact velocity, particle density and particle diameter are those for the base case.

Comparison of Figures 7 and 8 also shows the effect of the hindered settling on the higher volume fractions. The initial high volume fraction of particles in Figure 7 results in higher drag forces between the particles and the liquid, hindering the penetration of the particle plume. Whilst Figure 8 contains the same mass of particles as Figure 7, their introduction at a lower volume fraction has not caused hindered settling to have such an effect. Once the solids volume fraction increases beyond a value of approximately 0.2, the penetration of the particles is greatly reduced.

3.5 The Effect of Drag Coefficient Formulations and Mixture Viscosity

In this drag dominated flow, hindered settling, expressed by equations (1)-(2) has the expected result of decreasing the penetration of the particle plume, compared with the use of a single particle drag force. Comparison of Figure 2 with Figure 10, for which the drag coefficient is that for a single particle, shows the hindered settling effect at t = 0.15 s for the base case. The particles in Figure 10 have penetrated more deeply into the tank and are less compressed than those in Figure 2.

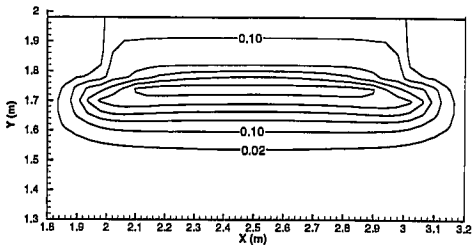

Figure 10
Contours of volume fraction for the base case at t = 0.15 s. The standard drag coefficient is applied. Contour values are 0.02, 0.1 - 0.5.

The solids viscosity formulation has little effect on the model performance. Contours of volume fraction are identical with and without solids viscosity, indicating that the viscous forces are small relative to the drag and gravity terms in the system.

4. CONCLUSIONS

The penetration of a stream of buoyant solids has been predicted numerically. As expected, an increase in the particle depth of penetration was achieved by an increase in impact

velocity, particle diameter and particle density and a decrease in inlet solids volume fraction. The time taken for particles to reach a volume fraction of 0.63 was found to increase with increased particle diameter and density, but decrease with increasing impact velocity and volume fraction.

Controlling the particle penetration depth has implications in a practical sense. In a metallurgical system, increasing the penetration depth can aid particle-slag penetration as well as the dispersion of the particles in the melt below. Delaying the accumulation of high volume fractions of particles is also of benefit since it allows greater access of the liquid to the particles, increasing the convective heat and mass transfer coefficients which in turn reduces particle dissolution time.

Modifications to the drag coefficient as given in equations (1) and (2), take into consideration the effects of particle packing. This resulted in the expected decrease in particle penetration with time due to the hindered settling effect.

The pronounced increase in particle depth with increasing particle diameter, compared with the effect of solids density variation, indicated the system to be drag rather than gravity dominated in the cases considered. The addition of a solids viscosity model had no effect, indicating that viscous effects play little part in this system.

ACKNOWLEDGMENTS

This work was funded by the Australian Government in the form of an Australian Postgraduate Award using facilities funded by the G.K. Williams Cooperative Research Centre for Extractive Metallurgy, a joint venture between the CSIRO Division of Minerals and the Department of Chemical Engineering, The University of Melbourne.

The authors would like to thank Dr. David Langberg for his useful discussions on the metallurgical implications of this work.

REFERENCES

AEA Technology, 1995, *CFX F3D User Guide*, Release 4.1, AEA Technology, Harwell Laboratory, Oxfordshire, UK.

Biswas, A.K., and Davenport, W.G., 1980, *Extractive Metallurgy of Copper*, Pergamon Press, Oxford, pp. 86-87.

Bouillard, J.X., Lyczkowski, R.W., and Gidaspow, D., 1989, "Porosity Distributions in a Fluidized Bed with an Immersed Obstacle", *AIChE Journal*, **35**, no. 6, June, pp. 908-923.

Brown, J.W., and Reddy, R.L., 1979, "Electric Arc Furnace Steel-Making with Sponge Iron", *Iron and Steelmaking*, **1**, pp. 24-31.

Davidson, M.R., 1994, "A Numerical Model of Liquid-Solid Flow in a Hydrocyclone with High Solids Fraction", *Numerical Methods in Multiphase Flow Proceedings of the 1994 ASME Fluids Engineering Division Summer Meeting*, **185**, Part 7, June 19-23, Lake Tahoe, p. 29-38.

Drew, D.A., and Lahey, R.T., 1987, "The Virtual Mass and Lift Force on a Sphere in Rotating and Straining Inviscid flow", *Int. J. Multiphase Flow*, **13**, pp. 113-121.

Errington, W.J., Fewings, J.H., Keran, V.P., and Denholm, W.T., 1985, "The Isasmelt Lead Smelting Process", *Extraction Metallurgy*, pp. 199-218.

Fletcher, D.F., and Witt, P.J., 1996, "Numerical Studies of Multiphase Mixing with Application to some Small-Scale Experiments", *Nuclear Engineering and Design*, **166**, pp. 135-145.

Fletcher, D.F., 1995, "Multiphase Mixing: Some Modelling Questions", *Int. Symp. on Two-Phase Flow Modelling and Experimentation*, Rome, Italy, 9-11 Oct., **2**, pp. 1005-1012.

George, D.B., and Taylor, J.C., 1981, *Copper Smelting- An Update*, The Metallurgical Society of AIME, pp. 96-97.

Gidaspow, D., 1986, "Hydrodynamics of Fluidization and Heat Transfer: Supercomputing Modelling", *Appl. Mech. Rev.*, **39**, pp. 1-23.

Gilbertson, M.A., 1993, "Mixing in Multiphase Jet Flow: Experimental Comparison with a Computational Model", *PhD Thesis*, University of Oxford, U.K.

Gilbertson, M.A., Fletcher, D.F., Hall, R.W., and Kenning, D.B.R., 1992, "Isothermal Coarse Mixing: Experimental and CFD Modelling", *IChemE Symp. Series*, **129**, pp. 547-556.

Griscom, F.N., 1994, and Lyles, D.R., "The FASTMET Process - Direct Reduction Technology for Modern Steelmaking", *Electric Furnace Conference Proceedings*, **52**, Nashville, Nov 13-16, pp. 75-81.

Guthrie, R.I.L., Clift, R., and Henein, H., 1975, "Contacting Problems Associated with Aluminum and Ferro-Alloy Additions in Steelmaking-Hydrodynamic Aspects", *Metallurgical Transactions B*, **6B**, June, pp. 321-329.

Hall, R.W., and Fletcher, D.F., 1995, "Validation of CHYMES: Simulant Studies", *Nuclear Engineering and Design*, **155**, pp. 97-114.

Incropera, F.P., and DeWitt, D.P., 1990, *Fundamentals of Heat and Mass Transfer*, John Wiley and Sons, Singapore, p. A13.

Kellogg, H.H., and Diaz, C., 1992, "Bath Smelting Processes in Non-Ferrous Pyrometallurgy: An Overview", *Proceedings of the Savard/Lee International Symposium on Bath Smelting*, pp. 39-65.

Lyczkowski, R.W., and Wang, C.S., "Hydrodynamic Modeling and Analysis of Two-Phase Non-Newtonian Coal Water Slurries", 1992, Powder Technology, 69, pp. 285-294.

Lyles, D.R., and Branning, G.S., 1992, "Effect on EAF Product Quality and Operating Efficiency of Using Direct Reduced Iron", *Electric Arc Furnace Conference Proceedings*, pp. 301-307.

Nagamori, M., Errington, W.J., Mackey, P.J., and Poggi, D., 1994, "Thermodynamic Simulation Model of the Isasmelt Process for Copper Matt", *Met. and Mat. Trans. B*, **25**, no. 6, Dec., pp. 839-853.

Peters, A.T., 1982, *Ferrous Production Metallurgy*, John Wiley and Sons, New York, pp. 109-110, 129-135.

Shook, C.A., and Roco, M.C., 1991, *Slurry Flow: Principles and Practice*, Butterworth-Heinemann, USA, pp. 62-63.

Stephenson, R.L. (Ed), 1980, *Direct Reduced Iron - Technology and Economics of Production and Use*, The Iron and Steel Society of AIME, pp. 120-121, 104-118.

van Leer, B., 1974, "Towards the Ultimate Conservative Difference Scheme. II. Monotonicity and Conservation Combined in a Second-Order Scheme", *Journal of Computational Physics*, **14**, pp. 361-370.

Zuber, N., 1964, "On the Dispersed Two-Phase Flow in the Laminar Flow Regime", *Chemical Engineering* Science, **19**, pp. 897-917.